

VELOCITY ESTIMATION OF GPS BASE STATIONS CONSIDERING COLORED NOISES

Weiwei Li^{1,2}, Yunzhong Shen¹

1Dept. of Surveying and Geo-informatics Engineering, Tongji University, Shanghai 200092, P.R. China; 2 Center for Spatial Information Science and Sustainable Development, Shanghai 200092, P.R. China

Email:whereareou@126.com

KEY WORDS: GPS monitoring series; impact analysis; common mode error; colored noise; w-test ;velocity

ABSTRACT:

In this paper, the noise characteristics of the GPS monitoring series of the base stations in China are analyzed and the velocities of these stations are estimated. The impacts of different error sources on velocity estimate are first analyzed. The results show that the unmodeled periodic signal will impact on the velocity estimate if the monitoring series is shorter than 4.5 years, and the impacts of white noise, flick noise and random walk noise are total different. Moreover, since the common mode error will influence the noise component estimates, the principal component analysis needs to be applied to extract the common mode errors from daily monitoring series, and then MINQUE needs to be used to correctly estimate the components of white noise and colored noises. The *w*-test is also adopted to determine the optimal stochastic model, which is the flick noise plus white noise, and the flick noise is apparently larger than white noise. Station velocities are then computed with optimal stochastic model, and the pure white noise model is also used to compute the station velocities as comparison. We processed 11 years data of the GPS monitoring series of 24 base stations in China with the above two models. The results show that the velocity uncertainty derived from optimal model is over 6 times larger than that derived from pure white noise model, which indicate that the pure white model get too optimistic velocity estimate. From the velocity estimates of the base stations, we can obviously get the tectonic motion trends.

1. INTRODUCTION

Common mode error (CME) is one of the spatially correlated error sources, which can be mitigated through regional filtering. Regional filtering was first introduced by Wdowinski et al (1997) to improve the resolution of coseismic and postseismic displacements in southern California. Assuming the CME spatially uniform, it is computed by the method called 'stacking' of the position residuals from linearly detrended time series. Nikolaidis (2002) employed the weighted stacking approach, which works well for regional networks such as SCIGN but has limitations when the network extends over larger regions. While, Dong et al (2006) raised a more rigorous approach without the assumption of spatially uniform, which is known as principal component analysis (PCA). PCA decomposes time series into a set of temporally modes and their spatial responses. The data themselves reveal the spatial distribution of the common mode error. The regional filtering has been widely used in studying various tectonics processes (Marquez-Azua and Demets, 2003; Wdowinski et al 2004).

Then, after regional filtering, the MLE (maximum likelihood estimation) method is generally used to compute the components of white noise, flick noise and random walk noise in the time series (Zhang et al, 1997; Langbein and Johnson, 1997; Mao et al, 1999; Williams et al, 2003; Langbein 2004). A.R.Amiri (2007) proposed the LS-VCE (Least squares variance component estimation), as the name describes, which is based on least squares method to assess the noise characteristics of the daily time series.

Moreover, Zhang et al (1997) deduced the expression of white noise, flick noise and random walk noise influenced on the velocity uncertainty. It suggested that the velocity error in coordinate time series may be underestimated by factors of 3-6 if pure white noise model is assumed according to the analysis

of 10 sites in southern California. Mao et al (1999) analyzed the 23 sites series with period of three years, which showed the factors of 5-11. Many researchers yield the similar conclusion (Yuan et al, 2008; Jiang et al, 2010; Tian et al, 2011), that is, the colored noises have effects on velocity error estimation.

Here, eleven years (1999-2009) GPS monitoring series of 24 base stations in China are processed. First, principal component analysis is employed in regional filtering. Then, MINQUE method is introduced to estimate the noise components due to the unbiased nature of it, and *w*-test is applied to determine the optimal noise model. Finally, station velocities are computed using the optimal noise model. The velocity estimates can reflect the motion trend of Mainland China.

2. IMPACT OF DIFFERENT ERROR SOURCES ON ESTIMATED VELOCITY

Just described as Nikolaidis (2002), the monitoring series of each station in each direction can be written as

$$y(t_i) = a + bt_i + \sum_{f=1}^2 (c_f \sin(2\pi ft_i) + d_f \cos(2\pi ft_i)) + \sum_{j=1}^{n_g} g_j H(t_i - T_{gj}) + \varepsilon_i \quad (1)$$

where, t_i ($i = 1, 2, \dots, m$) denotes the epoch in the units of years. a and b are the position and velocity of monitoring station, c and d describe periodic motion ($f = 1$ stands for the annual motion, $f = 2$ stands for the semi-annual motion).

The term $\sum_{j=1}^{n_g} g_j H(t_j - T_{gj})$ is used to correct the offsets,

which may arise from environmental and equipment changes or human intervention and error, with magnitudes g at epochs T_g , and H is the Heaviside step function. Equation (1) can be seen as the linear form of $\mathbf{x} = [a \ b \ c_1 \ d_1 \ c_2 \ d_2 \ g]$, so it can be described as

$$\mathbf{y} = \mathbf{A}\mathbf{x} + \boldsymbol{\varepsilon} \quad (2)$$

where, \mathbf{A} is the design matrix and assuming, $\boldsymbol{\Sigma}_y$ is the covariance matrix of \mathbf{y} . Then parameters can be estimated by using weighted least squares adjustment, that is,

$$\hat{\mathbf{x}} = (\mathbf{A}^T \boldsymbol{\Sigma}_y^{-1} \mathbf{A})^{-1} \mathbf{A}^T \boldsymbol{\Sigma}_y^{-1} \mathbf{y} \quad (3a)$$

And its covariance matrix is

$$\mathbf{Q}_{\hat{\mathbf{x}}} = \hat{\sigma}_0^2 (\mathbf{A}^T \boldsymbol{\Sigma}_y^{-1} \mathbf{A})^{-1} \quad (3b)$$

where, $\hat{\sigma}_0^2$ is the variance estimate of unit weight.

2.1 Impact of Unmodeled Periodic Signals

Assuming there is only one periodic signal and no offsets in monitoring series, then equation (1) can be simplified as

$$y(t_i) = a + bt_i + c_f \sin(2\pi ft_i) + d_f \cos(2\pi ft_i) + \varepsilon_i \quad (4)$$

According to Blewitt and Lavalée (2002), the velocity bias due to a sinusoidal signal can be expressed as

$$\hat{b}(T) = \frac{6p_f}{\pi f T^2} \left(\cos \pi f T - \frac{\sin \pi f T}{\pi f T} \right) \sin(\pi f T - \varphi) \quad (5)$$

where, T is the total span of the data; p_f is the amplitude of

the periodic signal, which equals to $\sqrt{c_f^2 + d_f^2}$, and the phase

φ equals to $\arctan\left(\frac{c_f}{d_f}\right)$. Since annual and semi-annual

signals are the two dominate signals in GNSS monitoring series, we only discuss these two periodic signals.

Figure 1 shows the theoretical bias for annual and semi-annual signals, respectively. And we assume the amplitude is 1mm and φ equals to $-\pi/2, 0, \pi/2, \pi$, respectively. It clearly

shows that the velocity biases become unstable when the time span is shorter than 2.5 years. And Blewitt and Lavalée gave a recommendation: as a practical rule, the minimum data span is 2.5 years for velocities estimated.

Equation (5) just reveals one periodic signal's impact on the velocity estimation. While to compute the velocity bias of a realistic repeating signal, the frequency has to be replaced by each harmonic of the fundamental frequency and each contribution has to be summed up.

Therefore, the velocity bias for a realistic repeating signal over time span T is given as

$$\hat{b}(T) = \sum_{k=1}^{1/(2f\Delta t)} \frac{6p_k}{\pi k f T^2} \left(\cos \pi k f T - \frac{\sin \pi k f T}{\pi k f T} \right) \sin(\pi k f T - \varphi_k) \quad (6)$$

Then Blewitt and Lavalée (2002) expressed the RMS velocity bias for a realistic repeating signal as

$$\sigma_{\hat{b}}(T) = \frac{6p_1}{\sqrt{2\pi} f T^2} \left(\sum_{k=1}^{1/(2f\Delta t)} \frac{1}{k^{2+\alpha}} \left(\cos \pi k f T - \frac{\sin \pi k f T}{\pi k f T} \right)^2 \right)^{\frac{1}{2}} \quad (7)$$

Figure 2 show the RMS velocity bias for the two periodic signals with different spectral indexes α (0, 1, 2). And the maximum Fourier component k is 183 for annual signal, 92 for semi-annual signal. It shows that RMS estimate rapidly decreases for data spans of 4.5 years or more. Whatever, the periodic signals have impact on the velocity estimation, especially for the data span shorter than 4.5 years. So it's better to simultaneously estimate the periodical signal if data span is shorter than 4.5 years.

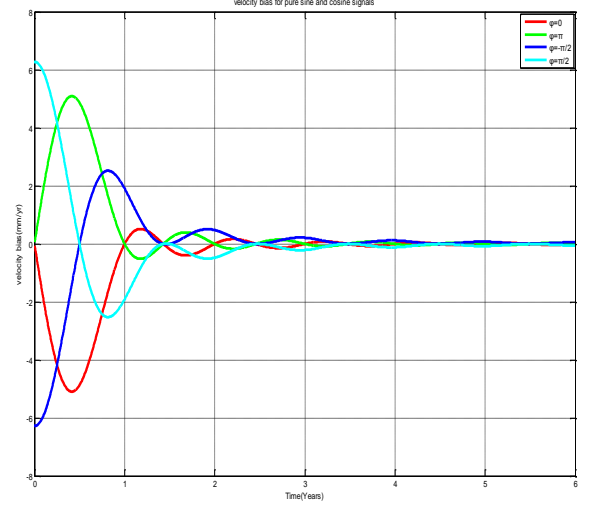


Figure1 (a). Theoretical velocity bias of annual signal

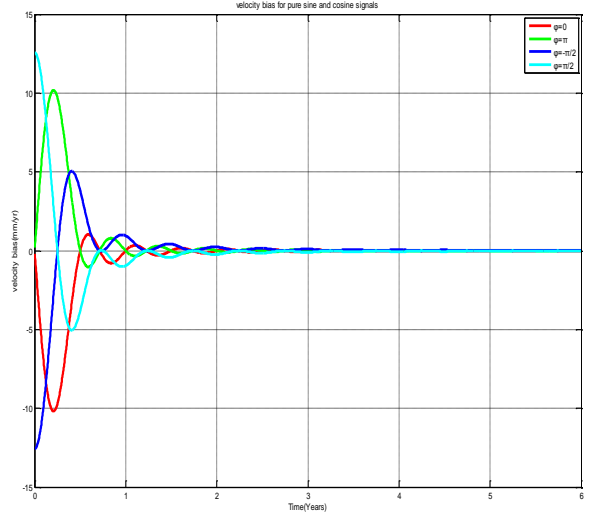


Figure1 (b). Theoretical velocity bias of semi-annual signal

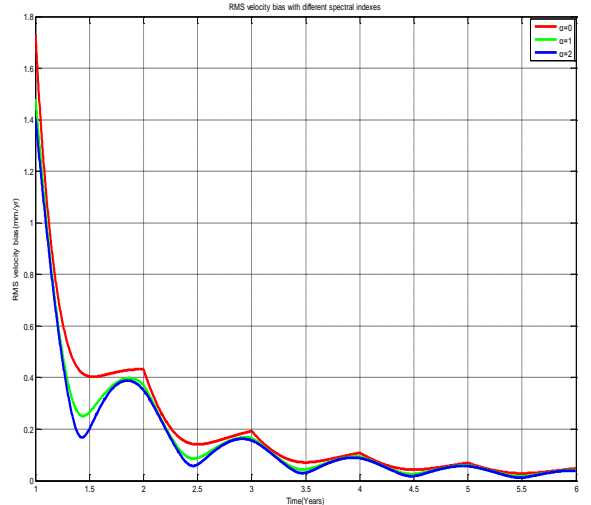


Figure 2(a). RMS velocity bias of annual series with different spectral indexes

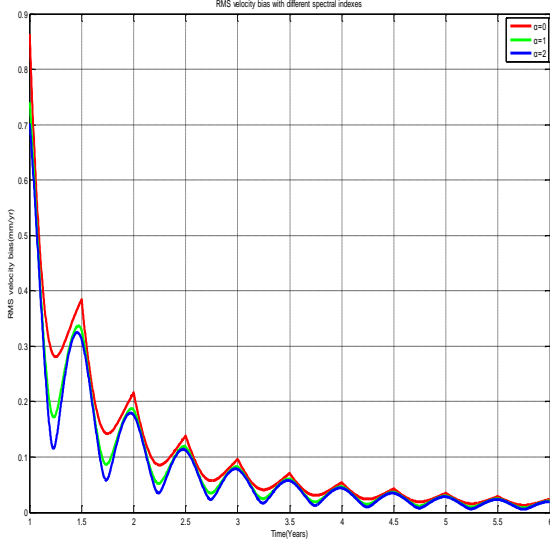


Figure 2(b). RMS velocity bias of semi-annual series with different spectral indexes

2.2 Impact of Different Noises

Zhang et al, Mao et al, William et al all presented the effect of colored noise on the velocity uncertainties. For white noise, the velocity uncertainty can be computed with

$$(\sigma_{\dot{r}}^2)_w = \frac{12\sigma_w^2}{\Delta t^2 m(m-1)(m+1)} \cong \frac{12\sigma_w^2}{mT^2} \quad (8)$$

For flick noise, the velocity uncertainty can be computed with

$$(\sigma_{\dot{r}}^2)_f = \frac{1.78\sigma_f^2 \Delta t^{0.22}}{T^2} \cong \frac{9\sigma_f^2}{16T^2} \quad (9)$$

For random walk noise, the velocity uncertainty can be computed with

$$(\sigma_{\dot{r}}^2)_{rw} = \frac{\sigma_{rw}^2}{\Delta t(m-1)} = \frac{\sigma_{rw}^2}{T} \quad (10)$$

where, $(\sigma_{\dot{r}}^2)_w, (\sigma_{\dot{r}}^2)_f, (\sigma_{\dot{r}}^2)_{rw}$ are velocity uncertainty that white noise, flick noise and random walk noise caused. T is the total observation span in years, Δt is sample interval, m is the observation number, $\sigma_w, \sigma_f, \sigma_{rw}$ is white, flick and random walk noise amplitudes respectively. Equations (8)-(10) are clearly show that different noises have different impact on velocity estimate. Therefore it is necessary to estimate the different noise components exactly.

2.3 Impact of Common Mode Error

For a regional network daily station coordinate monitoring series with n stations and spanning m days, the $m \times n$ matrix $X(t_i, x_j)$ ($i = 1, 2, \dots, m; j = 1, 2, \dots, n$) can be constructed. In the matrix X , each column contains a single coordinate components (north, east or vertical) of all epochs from a single station, and the each row contains coordinate components for all stations at a given epoch. It should be mentioned here that

the coordinate components are detrended and demeaned first. And the matrix X can be decomposed as

$$X(t_i, x_j) = \sum_{k=1}^n \mathbf{a}_k(t_i) \mathbf{v}_k(x_j) \quad (j = 1, 2, \dots, n) \quad (11)$$

$$\mathbf{a}_k(t_i) = \sum_{j=1}^n X(t_i, x_j) \mathbf{v}_k(x_j) \quad (k = 1, 2, \dots, n) \quad (12)$$

where, \mathbf{v}_k and \mathbf{a}_k is called the k th mode. If the eigenvalues are arranged in descending order, i.e. $\lambda_1 \geq \lambda_2 \geq \dots \geq \lambda_n$, the first principal component corresponds to the biggest eigenvalue λ_1 and the elements of its eigenvector \mathbf{v}_1 are close to each other. So it contains the most information of the monitoring series and with almost the same spatial response. Thus, common mode error (CME) can be expressed by

$$\boldsymbol{\varepsilon}_j(t_i) = \mathbf{a}_1(t_i) \mathbf{v}_1(x_j) \quad (13)$$

where, $\boldsymbol{\varepsilon}_j(t_i)$ denotes the error at epoch i for station j .

In regional network analysis, common mode error is the major spatially correlated error. Figure 3 shows the mean value of noise components of the GPS base stations in China before and after spatial filtering for white noise and flick noise. We can see that noise components of the filtered series are much smaller than that of the unfiltered, especially the flick noise.

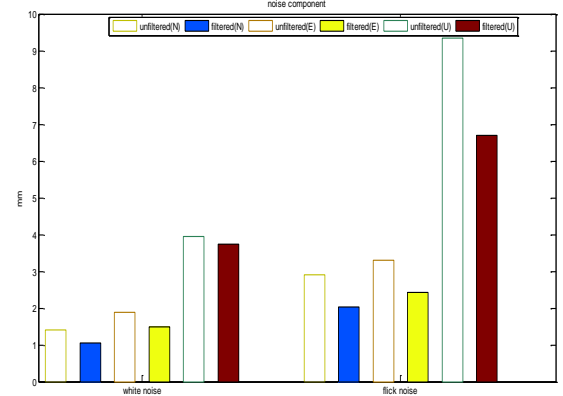


Figure 3. Noise component of unfiltered and filtered series

3. VELOCITY ESTIMATION OF GPS BASE STATION

3.1 Noise Component Estimation

The fundamental matrix equations for the iterative VCE (Li et al., 2010) is

$$\mathbf{R}_0 \boldsymbol{\Sigma}_y \mathbf{R}_0^T = \mathbf{v}_0 \mathbf{v}_0^T \quad (14)$$

where, $\mathbf{R}_0 = \mathbf{I}_n - \mathbf{A}(\mathbf{A}^T \boldsymbol{\Sigma}_0^{-1} \mathbf{A})^{-1} \mathbf{A}^T \boldsymbol{\Sigma}_0^{-1}$, $\mathbf{v}_0 = \mathbf{R}_0 \mathbf{y}$, $\boldsymbol{\Sigma}_0$ is the approximation of $\boldsymbol{\Sigma}_y$, and the other symbols are the same as that in Equation (2) and (3).

We use the general structure of $\boldsymbol{\Sigma}_y$ as,

$$\boldsymbol{\Sigma}_y = \sum_{i=1}^p \mathbf{U}_i \theta_i = \mathbf{Q} \boldsymbol{\theta}$$

where, θ_i is the i th unknown variance or covariance component and U_i is the given matrix for the component. The matrix equation (14) can be transformed into vector equations as

$$\mathbf{M}_0 \boldsymbol{\theta} = \text{vec}(\mathbf{v}_0 \mathbf{v}_0^T)$$

where, $\mathbf{M}_0 = [\text{vec}(\mathbf{R}_0 \mathbf{U}_1 \mathbf{R}_0^T) \cdots \text{vec}(\mathbf{R}_0 \mathbf{U}_p \mathbf{R}_0^T)]$ and $\text{vec}(\bullet)$ denotes the vector that converts a matrix to a column vector by stacking one column of the matrix underneath the previous one. Then the LS criterion is used on the vector equations with the weight matrix $\boldsymbol{\Sigma}_0^{-1} \otimes \boldsymbol{\Sigma}_0^{-1}$ to derive the VCE equation as

$$\mathbf{N} \hat{\boldsymbol{\theta}} = \mathbf{q} \quad (15)$$

The elements of matrix \mathbf{N} and vector \mathbf{q} are n_{ij} and q_i , respectively, which are expressed as

$$n_{ij} = \text{tr}(\mathbf{W}_0 \mathbf{U}_i \mathbf{W}_0 \mathbf{U}_j) \quad q_i = \mathbf{v}_0^T \mathbf{W}_0 \mathbf{U}_i \mathbf{W}_0 \mathbf{v}_0$$

where, $\mathbf{W}_0 = \mathbf{R}_0^T \boldsymbol{\Sigma}_0^{-1} \mathbf{R}_0 = \boldsymbol{\Sigma}_0^{-1} \mathbf{R}_0 = \mathbf{R}_0^T \boldsymbol{\Sigma}_0^{-1}$.

The iteration method is used to compute the noise component with the initial value $\boldsymbol{\Sigma}_0$.

3.2 Hypothesis Testing on Stochastic Model

Hypothesis testing is aimed to determine the appropriate noise model. The null hypothesis H_0 and the alternative hypothesis H_1 are constructed as follows,

$$H_0 : \boldsymbol{\Sigma}_y = \sigma_w^2 \mathbf{I} \quad H_1 : \boldsymbol{\Sigma}_y = \sigma_w^2 \mathbf{I} + \sigma_i^2 \mathbf{U}_i \quad (16)$$

where, \mathbf{U}_i is a known cofactor matrix of colored noise, σ_i is the component of colored noise, such as flick noise ($i = 2$) and random walk noise ($i = 3$). The w test model (A.R.Amiri,2007) can be presented as

$$\underline{w} = \frac{\mathbf{r} \hat{\boldsymbol{\epsilon}}^T \mathbf{U}_i \hat{\boldsymbol{\epsilon}} - \text{tr}(\mathbf{U}_i \mathbf{R}) \hat{\boldsymbol{\epsilon}}^T \hat{\boldsymbol{\epsilon}}}{\sigma_w^2 [2r^2 \text{tr}(\mathbf{U}_i \mathbf{R} \mathbf{U}_i \mathbf{R}) - 2r \text{tr}(\mathbf{U}_i \mathbf{R})]^2} \quad (17)$$

where, r is the redundancy of the functional model, which equals to $m - n$. $\hat{\boldsymbol{\epsilon}}$ is the least squares residuals under the null hypothesis, and \mathbf{R} refers to $\mathbf{I} - \mathbf{A}(\mathbf{A}^T \boldsymbol{\Sigma}_y^{-1} \mathbf{A})^{-1} \mathbf{A}^T \boldsymbol{\Sigma}_y^{-1}$. The distribution of \underline{w} , for large m , can be approximated by the standard normal distribution. The goal is to compute the statistic values for different alternative hypotheses and select the one that gives the maximum value for the hypothesis testing. The results in Appendix A suggest that white noise and flick noise model is the optimal model to describe the noise of monitoring series.

3.3 Estimation of Velocities

According to w test, the white noise plus flick noise model is superior to other models. Therefore, we use the optimal model to estimate the velocities of tectonic block movement. As a comparison we also compute it with pure white noise model. The covariance matrix of the optimal model is represented as

$$\boldsymbol{\Sigma}_y = \sigma_w^2 \mathbf{I} + \sigma_f^2 \mathbf{U}_2 \quad (18)$$

where, \mathbf{I} and \mathbf{U}_2 are the cofactor matrices of white noise and flick noise. According to Mao et al (1999), \mathbf{U}_2 can be approximated by

$$u_{ij} = \begin{cases} \left(\frac{3}{4}\right)^2 \times 2 & t_i = t_j \\ \left(\frac{3}{4}\right)^2 \times \left(2 - \frac{\log_{10} |t_i - t_j| / \log_{10} 2 + 2}{12}\right) & t_i \neq t_j \end{cases} \quad (19)$$

where, u_{ij} is the i row and j column element of matrix \mathbf{U}_2 . As comparison we also compute the velocities with pure white noise model, its covariance matrix is simplified from (18) as,

$$\boldsymbol{\Sigma}_y = \sigma_w^2 \mathbf{I}$$

Then weighted least squares adjustment is used to compute the velocities of tectonic block movement with 11 years monitoring series of 24 base stations in China. The distribution of these base stations and the estimated velocity vector are plotted in Figure 4, where the blue arrows stand for the velocities, while the red ellipses for the correspondent uncertainties. While the uncertainties are too small to display in the figure, it should be mention that the displayed uncertainties in Figure 4 are amplified by 25 and 2 times, respectively. The uncertainties computed with the optimal model are obviously larger than that with the pure white noise model, for detailed information one can refer to Appendix B1, which shows the enlarged factors of the uncertainties are from 6 to 16. As comparison the velocities of unfiltered series with the same two noise models are presented in Appendix B2. It is clear that CME also affect the estimated velocities. So CME should be extracted before parameters estimated.

It can be obviously seen from Figure 4 that the tectonic blocks of Mainland China has the obvious trend of moving towards eastern, although the details are not revealed since the base stations are too sparse.

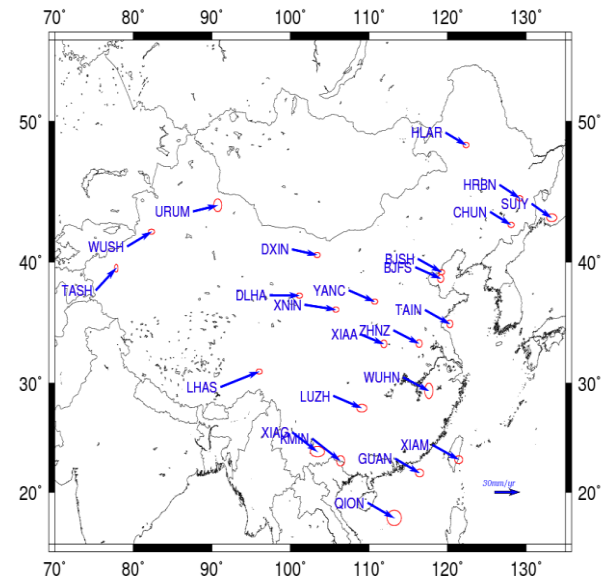


Figure 4(a). velocity field of Mainland China estimated with pure white noise

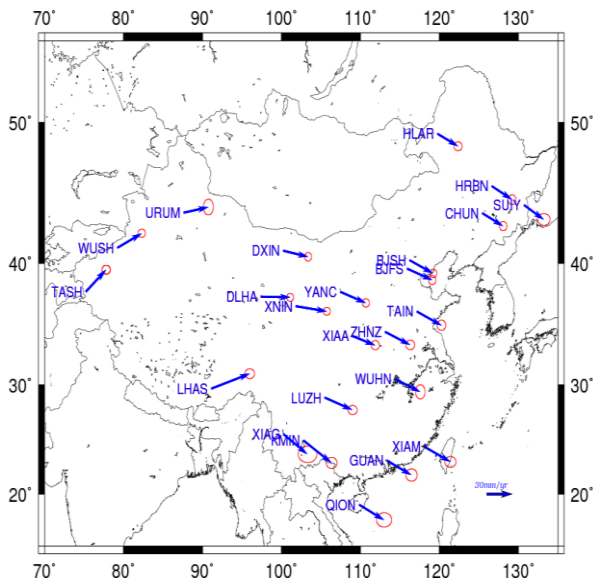


Figure 4(b). velocity field of Mainland China estimated with white noise and flick noise

4. CONCLUSION

We can draw the following conclusions from our theoretical analysis and numerical results:

- 1) Hypothesis testing shows that the dominate noises in GPS monitoring series are white noise plus flick noise. And the flick noise is even larger than white noise.
- 2) The impacts of periodic signal, colored noise and CME on velocity estimation should be taken into account. Therefore the CME must be filtered out and the colored noises must be estimated with proper method, such as MINQUE.
- 3) The tectonic blocks of Mainland China obviously move towards eastern. The stations in Qinghai-Tibetan Plateau have an obvious north-eastern movement; while in the east China, there is a clear south-eastern movement trend.

REFERENCE

A.R.Amiri-Simkoei, Least-Squares variance component estimation: theory and GPS applications, PHD Thesis, Delft university, 2007

Dong, P., Fang, Y., Bock, F., Webb, L., Prawirodirdjo, S., Kedar, and Jamason, Spatiotemporal filtering using principal component analysis and Karhunen-Loeve expansion approaches for regional GPS network analysis. *J. Geophys. Res.*, 2006, 111: 3405-3421.

Geoffrey Blewitt and David Lavallee Effect of annual signals on geodetic velocity. *Journal of geophysical research*, 2002, 107(B7), ETG9-1/9-11

Jiang Zhihao, Zhang Peng, Bi Jinzhong, Liu Lifen, Velocity estimation on the colored noise properties of CORS network in China based on the CGCS2000 Frame. *Acta Geodaetica et Cartographica Sinica*, 2010, 39(4), 355-363

Langbein, J., and H. Johnson. Correlated errors in geodetic time series: Implications for time-dependent deformation. *J. Geophys. Res.*, 1997, 102(B1): 591-603

Langbein, J. Noise in two-color electronic distance meter measurements revisited. *J. Geophys. Res.*, 2004, 109(B04406)

Li Bofeng, Shen Yunzhong and Lou Lizhi, Efficient Estimation of Variance and Covariance Components: A Case Study for GPS Stochastic Model Evaluation. *IEEE Transaction on Geoscience and Remot Sensing*, 2011, 49(1), 203-210

Mao A, Harrison C GA, Dixon T H. Noise in GPS coordinate time series. *J. Geophys. Res.*, 1999, 104(B2): 2797-2816

Marquez-Azua and Demets, B. and C. DeMets Crustal velocity field of Mexico from continuous GPS measurements, 1993 to June 2001: Implication for the neotectonics of Mexico. *J. Geophys. Res.* 2003, 108(B9), 2450

Rosanne Nikolaidis, Observation of Geodetic and Seismic Deformation with the Global Positioning System. San Diego: University of California, 2002

Tian Yunfeng, Shen Zhengkang, Li Peng, Analysis on correlated noise in continuous GPS observation, *Acta seismologica sinica*, 2011, 32(6), 696-704

Wdowinski, S., Y. Bock, J. Zhang, P. Fang and J. Genrich Southern California permanent GPS geodetic array: Spatial filtering of daily positions for estimating coseismic and postseismic displacements induced by the 1992 Landers earthquake. *J. Geophys. Res.* 1997, 102, 18057-18070

Wdowinski, S., Y. Bock, G. Baser, L. Prawirodirdjo, N. Bechor, S. Naaman, R. Knafo, Y. Forrai, and Y. Melzer, GPS measurements of current crustal movements along the Dead Sea Fault. *J. Geophys. Res.* 2004, 109, B05403

Williams S D P, Bock Y, Fang P, Jamason P, Nikolaidis R M, Prawirodirdjo L, Miller M, Johnson D J. Error analysis of continuous GPS position time series[J]. *J Geophys Res*, 2004, 109(B03412)

Yang Linguo, Ding Xiaoli, Chen Wu, Guo Zhihe, Chen Shaobin, Hong Benshan, Zhou Jintian, Characteristics of daily position time series from the Hong Kong GPS fiducial network[J], *Chinese Journal of Geophysics*, 2008, 51(5), P1372-1384.

Yunzhong Shen, Weiwei Li, Spatiotemporal related Signal and Noise Analysis of GPS Monitoring Series of the Base Stations in China, *IUGG 2011, June 28 2011 – July 9 2011, Melbourne, Australia*

Zhang, J., Y. Bock, H. Johnson, P. Fang, S. Williams, J. Genrich, S. Wdowinski, and J. Behr. Southern California Permanent GPS Geodetic Array: Error analysis of daily position estimates and site velocities. *J. Geophys. Res.*, 1997, 102(B8), 18035-18055

ACKNOWLEDGEMENT

The work was supported by the National Natural Science Funds of China (41074018, 40874016) and Kwang-Hua Fund for College of Civil Engineering, Tongji University. Data was provided by Crustal Movement Observation Network of China (CMONOC). The maps in this paper were generated using Generic Mapping Tools (GMT) software.

Appendix A
The statistic value of hypothesis test

Stations	N		E		U	
	WF	WR	WF	WR	WF	WR
BJFS	2239.7	621.6	1073.2	379.1	741.8	212.0
BJSH	1249.2	713.7	554.5	217.3	1397.2	434.3
TAIN	469.2	303.7	631.9	206.5	588.9	141.3
ZHNZ	932.8	474.7	1428.0	424.6	758.8	176.5
YANC	3446.2	1195.7	1712.1	644.7	1274.6	375.7
XIAA	2015.0	654.1	2423.2	598.5	654.1	144.5
CHUN	1387.4	752.1	893.6	147.6	1150.9	291.9
WUHN	1170.1	320.9	1324.4	311.7	1431.4	444.2
HRBN	1328.3	705.4	1346.7	131.9	5411.1	1178.0
HLAR	1000.5	529.7	1962.0	277.6	1876.0	311.5
XNIN	2606.4	867.1	2445.3	774.7	1690.4	446.8
DXIN	3275.6	60.3	2504.1	694.3	2054.2	464.8
SUIY	822.6	175.8	1439.2	240.2	181.7	18.3
LUZH	3597.5	1098.3	2250.1	721.1	603.8	140.9
DLHA	2451.4	909.3	2452.3	706.4	736.4	192.1
XIAM	712.2	282.9	1154.9	296.4	1575.9	461.4
GUAN	608.0	164.8	1063.1	207.1	495.4	86.9
KMIN	2391.8	863.5	434.2	92.2	698.9	155.1
XIAG	4803.4	985.6	1608.6	324.8	752.0	199.2
QION	498.3	92.7	911.0	209.0	300.1	80.6
URUM	2999.9	264.7	357.9	31.4	1623.1	91.0
LHAS	1038.7	274.0	1451.5	217.8	241.9	64.8
WUSH	512.9	147.8	1030.4	137.7	282.2	34.3
TASH	947.2	120.1	273.0	44.5	655.9	158.9

Appendix B1
Velocity estimation of filtered series under different noise model (mm/yr)

Station		Noise model				Amplification factor
		W		WF		
		velocity	SD	velocity	SD	
BJFS	N	-11.21	0.02	-11.30	0.17	8.50
	E	30.35	0.02	30.31	0.17	8.50
BJSH	N	-12.95	0.02	-12.91	0.13	6.50
	E	28.35	0.02	28.46	0.18	9.00
TAIN	N	-13.68	0.02	-13.59	0.16	8.00
	E	29.68	0.02	29.78	0.23	11.50
ZHNZ	N	-12.99	0.02	-12.80	0.17	8.50
	E	30.61	0.02	30.40	0.21	10.50
YANC	N	-11.04	0.01	-10.99	0.13	13.00
	E	30.92	0.01	30.93	0.12	12.00
XIAA	N	-9.31	0.02	-9.10	0.18	9.00
	E	27.25	0.02	27.45	0.19	9.50
CHUN	N	-12.75	0.02	-12.69	0.19	9.50
	E	25.05	0.02	25.11	0.23	11.50
WUHN	N	-13.57	0.05	-12.66	0.35	7.00
	E	30.56	0.03	30.62	0.28	9.33
HRBN	N	-12.98	0.02	-12.85	0.21	10.50
	E	24.22	0.02	24.4	0.27	13.50
HLAR	N	-12.06	0.02	-11.95	0.20	10.00
	E	24.64	0.02	24.84	0.27	13.50
XNIN	N	-4.96	0.01	-4.94	0.12	12.00
	E	37.31	0.02	37.24	0.14	7.00
DXIN	N	-5.73	0.01	-5.84	0.19	19.00
	E	29.99	0.02	30.03	0.17	8.50
SUIY	N	-13.80	0.02	-13.89	0.30	15.00
	E	23.88	0.04	23.82	0.48	12.00
LUZH	N	-11.93	0.02	-11.81	0.17	8.50
	E	33.62	0.02	33.43	0.17	8.50
DLHA	N	-0.50	0.01	-0.54	0.14	14.00
	E	35.36	0.02	35.20	0.16	8.00
XIAM	N	-14.30	0.02	-14.36	0.25	12.50
	E	31.30	0.03	31.42	0.32	10.67
GUAN	N	-14.07	0.02	-14.01	0.31	15.50
	E	29.43	0.04	29.69	0.42	10.50
KMIN	N	-21.44	0.03	-21.47	0.22	7.33
	E	33.82	0.04	33.79	0.33	8.25
XIAG	N	-18.86	0.04	-19.33	0.46	11.50
	E	29.43	0.05	28.94	0.56	8.88

QION	N	-15.00	0.05	-14.66	0.38	7.60
	E	31.19	0.05	29.93	0.44	8.80
URUM	N	5.65	0.05	5.25	0.48	9.60
	E	29.51	0.04	29.64	0.40	10.00
LHAS	N	14.52	0.02	14.27	0.25	12.50
	E	46.23	0.03	46.15	0.33	11.00
WUSH	N	13.80	0.02	13.74	0.22	11.00
	E	29.29	0.03	29.36	0.28	9.33
TASH	N	20.90	0.02	20.92	0.27	13.50
	E	24.38	0.03	24.28	0.33	11.00

Appendix B2

Velocity estimation of unfiltered series under different noise model (mm/yr)

Station		Noise model				Amplification factor
		W		WF		
		velocity	SD	velocity	SD	
BJFS	N	-10.88	0.03	-10.95	0.30	10.00
	E	30.68	0.03	30.25	0.29	9.67
BJSH	N	-12.70	0.02	-12.66	0.28	14.00
	E	28.58	0.03	28.41	0.29	9.67
TAIN	N	-13.39	0.03	-13.30	0.33	11.00
	E	29.98	0.03	29.72	0.36	12.00
ZHNZ	N	-12.71	0.03	-12.52	0.31	8.50
	E	30.99	0.03	30.32	0.36	10.33
YANC	N	-10.76	0.02	-10.69	0.27	13.50
	E	31.22	0.03	30.87	0.29	9.67
XIAA	N	-9.07	0.03	-8.85	0.30	10.00
	E	27.54	0.03	27.40	0.33	11.00
CHUN	N	-12.51	0.02	-12.43	0.30	15.00
	E	25.22	0.03	25.07	0.30	10.00
WUHN	N	-12.99	0.06	-12.37	0.46	7.67
	E	30.95	0.04	30.55	0.39	9.75
HRBN	N	-12.73	0.02	-12.59	0.32	16.00
	E	24.39	0.03	24.35	0.32	10.67
HLAR	N	-11.83	0.02	-11.71	0.29	14.50
	E	24.83	0.03	24.80	0.33	11.00
XNIN	N	-4.69	0.02	-4.65	0.25	12.50
	E	37.61	0.03	37.17	0.29	9.67
DXIN	N	-5.45	0.02	-5.54	0.28	14.00
	E	30.29	0.03	29.97	0.28	9.33
SUIY	N	-13.47	0.03	-13.56	0.38	12.67
	E	24.07	0.05	23.90	0.50	10.00
LUZH	N	-11.62	0.03	-11.48	0.30	10.00
	E	34.15	0.05	33.38	0.37	7.40
DLHA	N	-0.27	0.02	-0.28	0.26	13.00
	E	35.66	0.03	35.14	0.28	9.33
XIAM	N	-13.97	0.03	-14.02	0.35	11.67
	E	31.72	0.04	31.35	0.46	11.50
GUAN	N	-13.81	0.03	-13.73	0.40	13.33
	E	29.52	0.04	29.68	0.46	11.50
KMIN	N	-21.20	0.04	-21.19	0.36	9.00
	E	34.05	0.04	33.73	0.44	11.00
XIAG	N	-18.48	0.04	-18.90	0.53	13.25
	E	30.11	0.07	28.80	0.76	10.86
QION	N	-14.59	0.06	-14.26	0.46	7.67
	E	31.97	0.07	29.86	0.62	8.86
URUM	N	5.75	0.05	5.42	0.51	10.20
	E	29.57	0.04	29.63	0.41	10.25
LHAS	N	14.71	0.03	14.49	0.32	10.67
	E	46.49	0.03	46.10	0.39	13.00
WUSH	N	13.96	0.02	13.92	0.27	13.50
	E	29.39	0.03	29.34	0.30	10.00
TASH	N	21.02	0.02	21.06	0.29	14.50
	E	24.48	0.03	24.27	0.34	11.33

W: white noise

WF: white noise and flick noise

WR: white noise and random walk noise

SD: standard deviation